Progress In Electromagnetics Research C, Vol. 95, 183–194, 2019

Staircase Fractal Loaded Microstrip Patch Antenna for Super Wide Band Operation

Swarup Das*, Debasis Mitra, and Sekhar R. B. Chaudhuri

Abstract—In this paper a staircase fractal curve is applied on a microstrip line fed truncated corner square patch antenna to achieve Super Wide Band (SWB) operation. The proposed antenna exhibits an impedance bandwidth from 0.1 GHz to 30 GHz with a ratio impedance bandwidth of 300 : 1 for $S_{11} \leq -10$ dB. The bandwidth enhancement of the proposed antenna structure due to the fractal curve is shown in a step by step manner. The Bandwidth Dimension Ratio (BDR) of the proposed antenna design is obtained as 496675. Relatively stable omnidirectional radiation pattern and satisfactory value of gain are obtained over the operation band. Time domain analysis has also been performed to check the applicability of the proposed design as SWB antenna.

1. INTRODUCTION

In the recent time there is a huge development in the field of wireless communication systems. Owing to this development the demand for compact antennas capable of operating at an extremely wide frequency band with high data rate transmission is also increasing. There are ultra-wideband antennas (3.1–10.6 GHz) for short range communications, but WPAN (Wireless Personal Area Network) users want an antenna which covers both short and long range communications. To fulfil this requirement, the concept of super wideband antenna comes into the existence. Super wideband (SWB) antennas are the antennas which support more than decade bandwidth (10 : 1 or more) at $S_{11} \leq -10$ dB [1]. Different techniques have been utilized in designing these types of planar, low profile compact antennas which can support SWB operation [2–21].

A tapered coplanar waveguide (CPW) fed elliptical monopole patch antenna with trapezoidal ground plane has been reported in [2] for SWB operation. Further bandwidth enhancement of similar type of patch antenna has been observed in [3] using tapered microstrip feedline integrated with a semi ring feeding structure. A tapered microstrip fed patch made of one half disc and one half ellipse with a corner rounded ground plane has been presented in [4] as SWB antenna. A planar circular asymmetric dipole antenna structure has been reported in [5] which exhibits a ratio impedance bandwidth of 21.9 : 1. Dual branch feed with an L-shaped feed branch has been utilized for SWB operation of a modified rectangular patch antenna in [6]. A semi-circular shaped and a tapered shaped SWB patch antennas have been reported in [7] and [8] respectively where a tapered feed line is used for bandwidth enhancement. Similarly in [9], a tapered line fed tapered shaped patch antenna with chamfered ground plane has been presented which shows an impedance bandwidth ratio of 111.1 : 1. In [10] reactive loading technique has been applied on a patch antenna to achieve required bandwidth for SWB operation. A tapered microstrip line fed circular base loaded modified rectangular monopole antenna is designed in [11] which exhibits an impedance bandwidth ratio of 14.56 : 1. In [12] A CPW fed modified square monopole antenna has been reported for SWB operation. A crescent shaped microstrip patch antenna

Received 1 July 2019, Accepted 26 August 2019, Scheduled 8 September 2019

* Corresponding author: Swarup Das (dasswarup08@yahoo.in).

The authors are with the Electronics and Telecommunication Engineering Department, Indian Institute of Engineering Science and Technology, Shibpur, Howrah 711103, West Bengal, India.

with a partial ground plane has been proposed in [13] which shows an impedance bandwidth ratio of 11.6 : 1. In [14] a tapered triangular microstrip line fed trapezoidal patch antenna with semicircular ground plane has been reported for SWB operation.

Application of fractal geometry in a planar antenna structure has been accepted as one of the important techniques for bandwidth enhancement. Fractal is a geometric shape that can be segmented into different parts, and each part is the copy of the whole for which we get two properties of self similarity and space filling which lead to multiband and miniaturization of the antenna, respectively. The fractal antennas can generate several resonant bands, and those bands may be combined to obtain SWB operation. Application of different fractal geometries on planar antennas for SWB operation has been shown in [15–21]. In [15] semi-elliptical fractal slots are etched on the ground plane of an egg shaped monopole antenna to achieve SWB operation. A modified star triangular fractal antenna has been presented in [16] for SWB application. A microstrip line fed modified star star fractal antenna with notch loaded semi-elliptical ground plane has been reported in [17] for SWB application. A CPW-fed hexagonal Sierpinski fractal antenna has been designed in [18] which exhibits an impedance bandwidth ratio of 11 : 1. In [19] an SWB antenna has been designed using a complimentary Sierpinski triangle surrounded by two semi-circular sectors. A circular hexagonal fractal antenna and circle inscribed hexagonal fractal antenna have been designed in [20] and [21] to achieve an impedance bandwidth ratio of 20.4 : 1 and 25.82 : 1, respectively. Likewise, recently a hexagonal triangular fractal antenna [22] and a square inscribed circular fractal antenna [23] have been reported for wideband application which show an impedance bandwidth ratio of 8.4 : 1 and 7.17 : 1, respectively.

In all these reported antennas bandwidth dimension ratio (BDR) is an important factor which signifies the fractional bandwidth (in %) per unit electrical area of the antenna. This electrical area is represented in terms of wavelength which corresponds to the lower edge frequency of SWB operation. Therefore if lower edge frequency is reduced, then the fractional bandwidth will increase, and the corresponding wavelength will also be higher as the lower edge frequency decreases. Now when the physical area of the antenna structure is expressed in terms of that wavelength the corresponding electrical area will decrease. As a result, a high value of BDR will be obtained which indicates more bandwidth with comparatively smaller size of antenna.

In this paper a staircase fractal curve is applied on a microstrip line fed truncated corner square patch antenna fabricated on a $60 \times 60\,\text{mm}^2$ FR4 substrate. It exhibits an impedance bandwidth from 0.1 GHz to 30 GHz. As the lower edge frequency of SWB operation is significantly reduced a high value of BDR, i.e., 496675, is obtained. The proposed antenna structure is simulated using Finite Element Method based HFSS13 software. The antenna prototype is fabricated, and different antenna parameters are measured. The comparison of the various parameters of the proposed design with other reported designs is also presented. A detailed time domain analysis of the proposed antenna design is also performed to confirm its application as SWB antenna.

2. ANTENNA DESIGN

The configuration of the proposed SWB antenna labelled with the design parameters is shown in Figure 1. The antenna is designed on a $60 \times 60\,\text{mm}^2$ ($L_S \times W_S$) FR4 substrate with dielectric constant 4.4 (ϵ_r) and thickness 1.6 mm (h). The optimized length (L_F) and width (W_F) of the microstrip feed line are chosen as 8 mm and 3 mm respectively to achieve 50 Ω impedance matching. On the opposite side of the FR4 substrate a partial ground plane of length 7.5 mm (L_G) is utilized for wide band operation. Initially a square patch of side length $W = 40$ mm is designed as a radiating element. Then two lower corners of the square patch are modified by etching two triangular sections from the patch. The height and base of the triangular sections are given by $L_C = 9$ mm and $W_C = 18.5$ mm respectively. Therefore, the modified length of the patch is $L = (W - L_C) = 31$ mm. To achieve SWB operation three identical staircase fractal curves of fifth order iteration are added along the two side edges and top edge of the modified patch. Along the side edges of the patch the generation of staircase fractal curve starts with a rectangle of width $q = 2$ mm on both side of the patch. These rectangles are placed at a same distance of $p = 2$ mm from the top corner as well as from the bottom corner. In the second iteration rectangles of same width are placed at a same distance from top as well as bottom side. This process is repeated up to the fifth iteration of staircase fractal curve. Apart from side edges rectangles are added in a

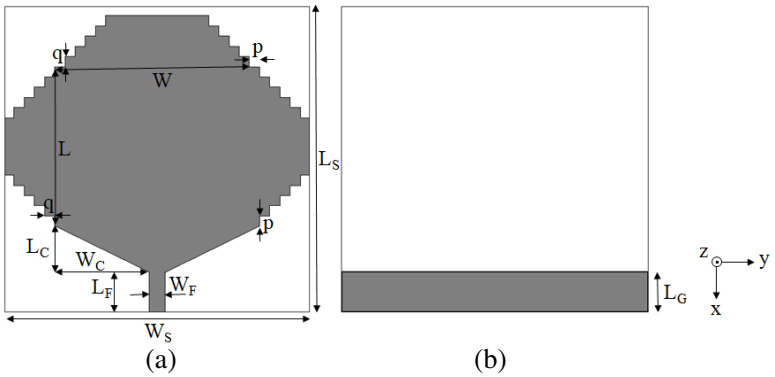

Figure 1. Geometry of the proposed SWB antenna. (a) Top view. (b) Bottom view.

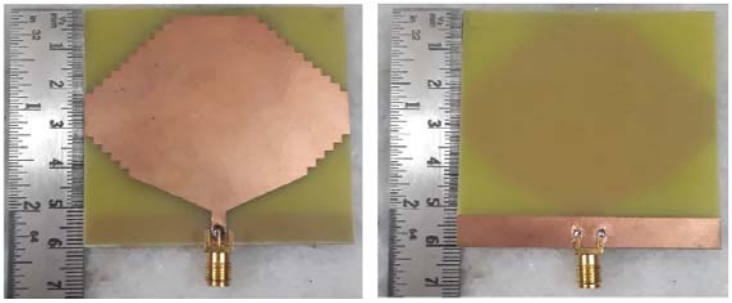

Figure 2. Photograph of the fabricated prototype of the proposed SWB antenna. (a) Top view. (b) Bottom view.

similar manner along the top edge also. Initially the first rectangle is placed at a distance of $p = 2\,\text{mm}$ from both side, and the width of the rectangle is kept at $q = 2\,\text{mm}$. This process of adding rectangle at top edge in the form of staircase is repeated in the subsequent iterations of staircase fractal curve generation. Both side photographs of the fabricated prototype of the proposed SWB antenna are shown in Figure 2.

3. RESULTS AND DISCUSSIONS

Initially the square microstrip patch antenna is simulated which shows poor impedance matching especially in lower frequency range as shown in Figure 3. It happens due to the abrupt truncation of feed line at the straight base of square shaped radiating element [12]. To improve the impedance matching two triangular sections are etched from the two lower corners of the square patch. As a result, a gradual change in impedance at the junction of feed point and square patch improves matching at lower frequency range. The corner modified microstrip patch antenna shows an impedance bandwidth from 0.75 GHz to 30 GHz with a small mismatching around 5 GHz as shown in Figure 3. The lower edge frequency of this patch antenna can be calculated from the following equations [11].

$$f_L = \frac{7.2}{(W + r + g)\sqrt{\epsilon_{eff}}} \tag{1}$$

Here W = side length of square patch, $r = \frac{W}{2\pi}$ and g = gap between square patch and ground plane=$(L_F - L_G) = (8 - 7.5)\,\text{mm} = 0.5\,\text{mm}$.

$$\epsilon_{eff} = \frac{\epsilon_r + 1}{2} + \frac{\epsilon_r - 1}{2}\left(1 + 12\frac{h}{W}\right)^{-\frac{1}{2}} \tag{2}$$

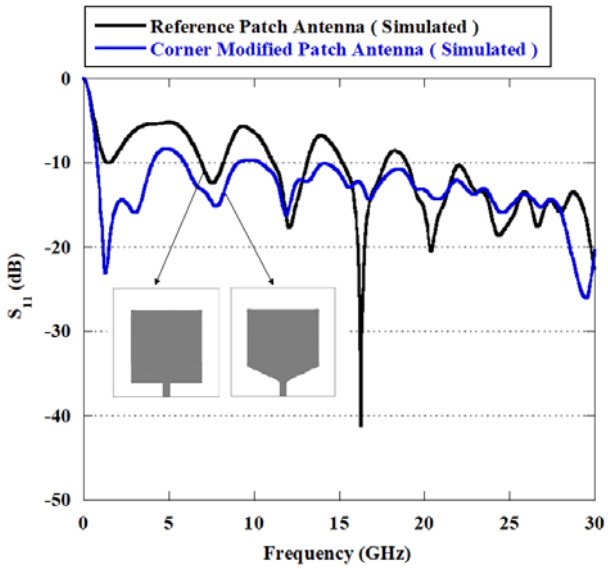

Figure 3. Reflection Coefficient plot for Square and Corner modified patch antenna.

After substituting all the parameters the value of ϵ_{eff} is obtained as 4.1 from Eq. (2). In Eq. (1) the values of W, r and g are substituted in cm. After substituting all the parameters the lower edge frequency is obtained as 0.76 GHz from Eq. (1).

In Figure 4 different iterative stages of staircase fractal loaded antenna structures are depicted. In the first iterative structure the lower edge frequency of operation is reduced to 0.69 GHz, and the entire band is obtained upto 30 GHz with a small mismatching around 5 GHz as shown in Figure 5. In the second iteration stage the bandwidth is obtained from 0.61 GHz to 30 GHz with very small mismatching around 11 GHz, 14.5 GHz, and 19.68 GHz. In the next iteration the lower edge frequency of operation is further reduced to 0.55 GHz, and a very small mismatching is observed around 10.37 GHz. In the fourth iterative structure the entire bandwidth is obtained from 0.5 GHz to 30 GHz without any mismatching as shown in Figure 6. In the final iteration stage lower edge frequency is further reduced to 0.09 GHz, and the entire bandwidth is obtained up to 30 GHz. The reflection coefficient of the final iterative structure is measured using a Rohde & Schwarz Vector Network Analyzer. The measured result shows an impedance bandwidth from 0.1 GHz to 30 GHz. In this manner the miniaturization property of fractal curve is utilized to reduce the lower edge frequency of operation which in turn increases the bandwidth dimension ratio (BDR) of the proposed SWB antenna structure.

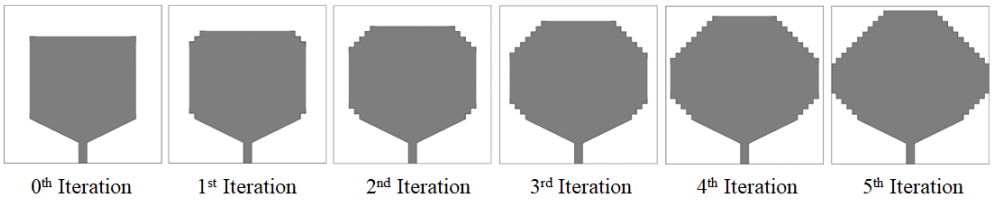

Figure 4. Different stages of iteration for staircase fractal loaded antenna.

The total increase in patch length, i.e., the distance between the bottom corner and top corner of the patch can be calculated for each stage of iteration. In the first order iteration when a single rectangle is added total increase in distance along the side edge of the patch is $2q$ and along top edge is q as per the dimensions given in Figure 1. So the net increase in distance is $3q$ in the first iterative structure. Similarly in each subsequent stage of iteration, the total increase in distance is $3q$. Therefore at the end of the fifth iteration the total increase in distance is $(5 \times 3q) = 15q = (15 \times 2)\,\text{mm} = 30\,\text{mm}$.

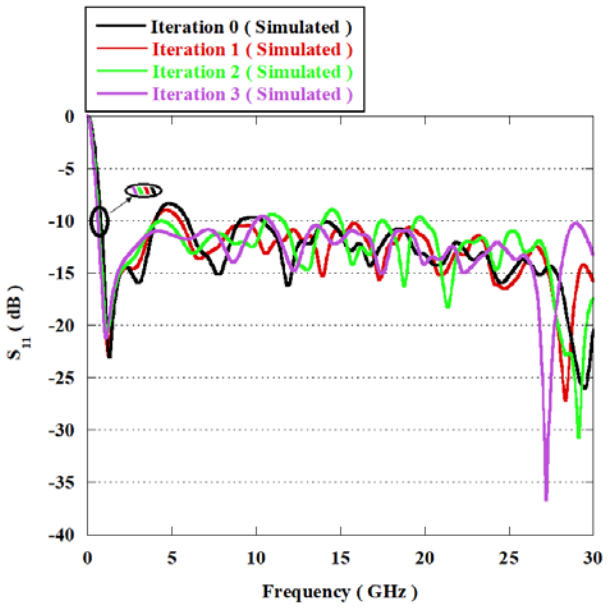

Figure 5. Reflection Coefficient plot for 0^{th} to 3^{rd} order iterative structure.

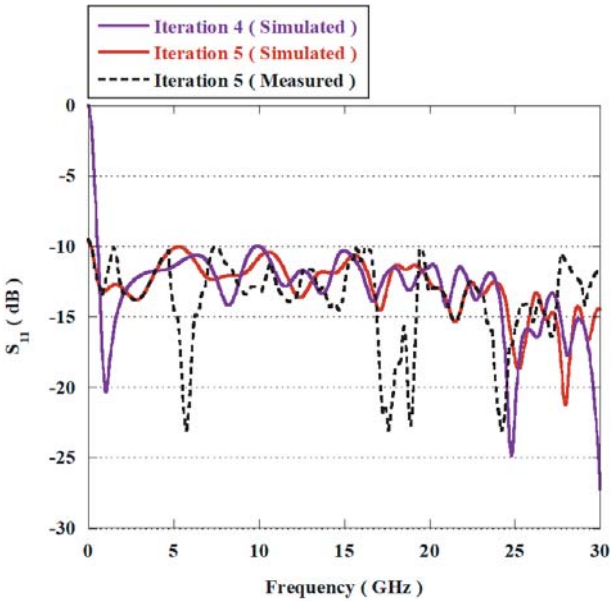

Figure 6. Reflection Coefficient plot for 4^{th} and 5^{th} order iterative structure.

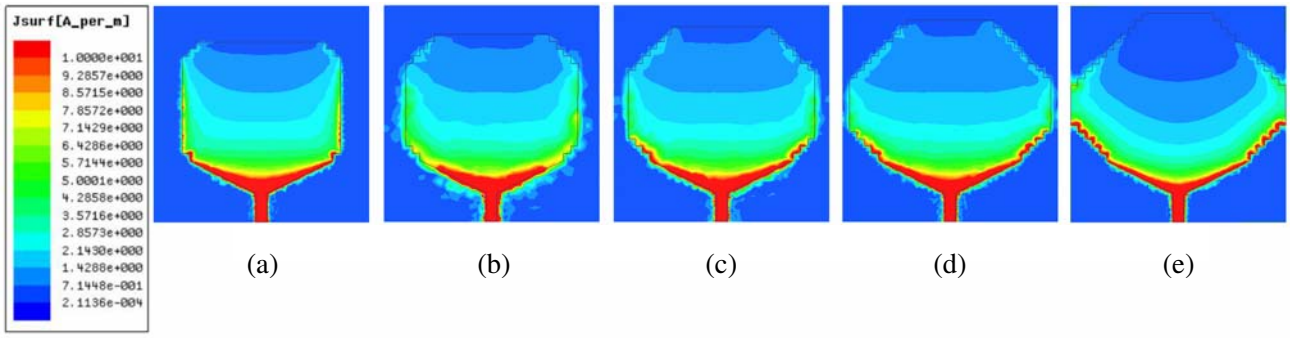

Figure 7. Surface current distributions at (a) 0.69 GHz, (b) 0.61 GHz, (c) 0.55 GHz, (d) 0.5 GHz, (e) 0.09 GHz.

Likewise, the width in each stage of iteration along the side edges of the patch is enhanced by a distance of $2q$. So at the final stage of iteration the increase in width is $(5 \times 2q) = 10q = (10 \times 2)\,\text{mm} = 20\,\text{mm}$. This enhancement of patch size along both vertical and horizontal directions results in the reduction in lower edge frequency of operation and SWB operation is obtained.

The surface current distribution of different iterative antenna structures at their respective lower edge frequency of operation is shown in Figure 7. As the order of iteration increases the surface current path length also increases. Therefore, the lower edge frequency of operation decreases with increase in subsequent iteration stages. Finally in the fifth iteration stage when the side edges of the patch touch the substrate edge the penetration of the surface current around the edges of the patch is more than previous cases. As a result, the decrease in lower edge frequency of operation is also higher than previous stages.

Figure 8 demonstrates the real and imaginary parts of the input impedance of the final proposed SWB antenna structure. It is observed that the real and imaginary parts of the input impedance vary around $50\,\Omega$ and $0\,\Omega$ respectively over the entire frequency range of operation. These variations provide an approximate input impedance of $50\,\Omega$ and good impedance matching with the characteristics impedance of SMA connector, i.e., $50\,\Omega$ is obtained. Therefore, reduced value of reflection coefficient

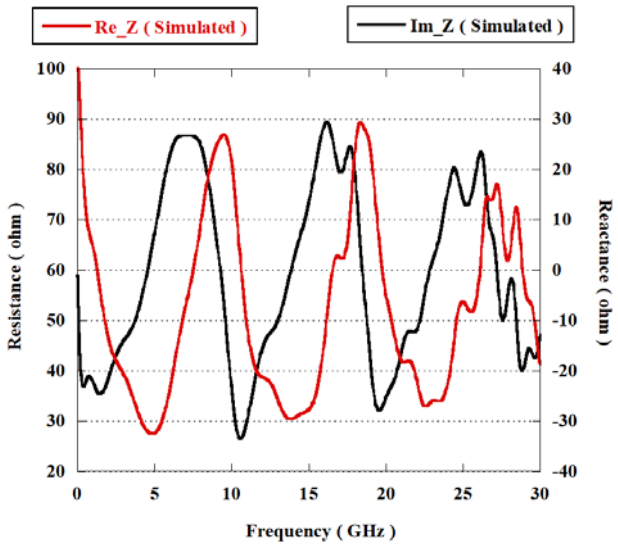

Figure 8. Real and Imaginary part of the input impedance of final proposed antenna structure.

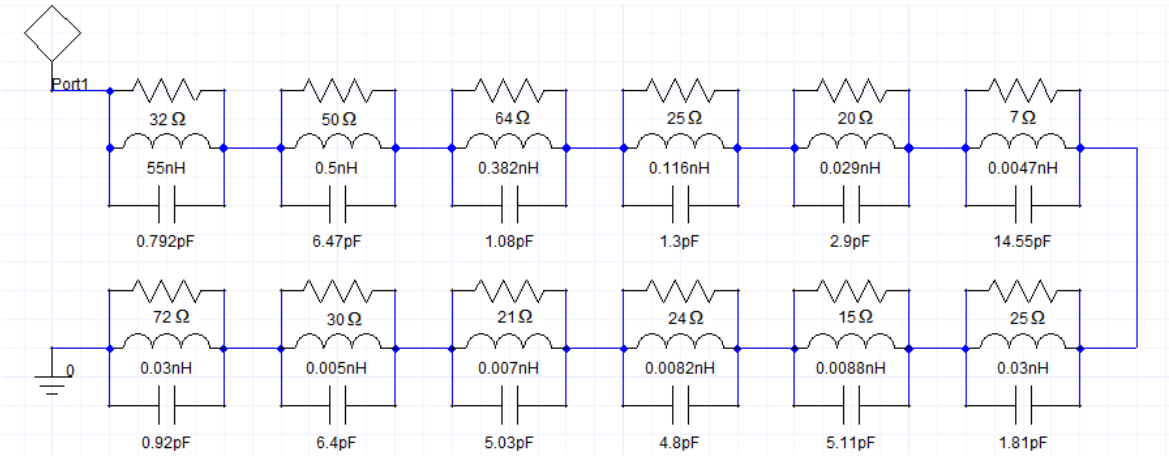

Figure 9. Equivalent circuit model of the proposed SWB antenna.

(S_{11}) is found over the entire frequency band of SWB operation.

An equivalent circuit model of the proposed SWB antenna is presented in Figure 9. In this model the reflection coefficient characteristics can be achieved due to several resonances of the proposed antenna structure where each resonance is modelled as a parallel RLC circuit [9]. The reflection coefficient plot of the proposed antenna design shows twelve prominent resonant frequencies as obtained from HFSS simulation. Based on this, twelve parallel RLC circuits are designed which are connected in a series connection. The resonant frequency of a parallel RLC circuit is given by $f_r = \frac{1}{2\pi\sqrt{LC}}$, and the Q factor is given by $Q = R\sqrt{\frac{C}{L}}$. Accordingly the values of Resistance (R), Inductance (L) and Capacitance (C) are chosen for each RLC circuit to control the resonant frequency and the bandwidth along with level of S_{11}. However as the entire band is continuous and response of one RLC circuit affects the neighbour RLC circuit, some modifications in those values are also made when required. The staircase fractal structure is formed by introducing rectangular metallic portions one after another which is considered equivalent to increase in the effective value of inductance. Therefore in the first RLC circuit comparatively high value of inductance is chosen which reduces the first resonant frequency and the lower edge frequency of operation. As a result, the required impedance bandwidth is obtained for the SWB operation. The

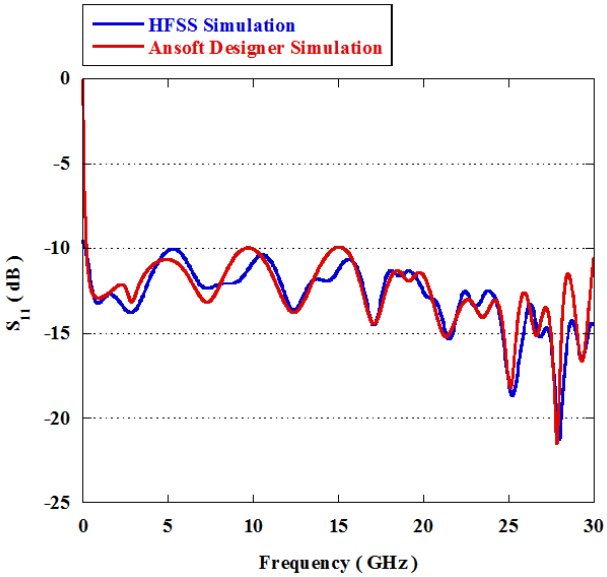

Figure 10. Reflection coefficient plot for proposed SWB antenna and its equivalent circuit model.

equivalent circuit model is designed and simulated using Ansoft Designer software. The optimized values of R, L, and C are shown in Figure 9. The simulated response of this proposed equivalent circuit model is depicted in Figure 10.

Bandwidth Dimension Ratio (BDR) is an important parameter of SWB antenna. BDR is defined as operating bandwidth per electrical area of the antenna structure. It is calculated from the following equation [16]

$$\text{BDR} = \frac{\text{Bandwidth}(\%)}{\lambda_{\text{length}} \times \lambda_{\text{width}}} \tag{3}$$

Here λ_{length} and λ_{width} are the length and width of the proposed antenna design in terms of λ where λ corresponds to the wavelength of the lower edge frequency of operation. As the lower edge frequency of operation decreases the corresponding value of λ increases. Therefore, the length and width of the proposed design in terms of λ decrease. Here from S_{11} plot the bandwidth obtained is 198.67%. The length and width in terms of λ of the proposed antenna structure are same, i.e., 0.02λ. After substituting all these values in Eq. (3) the value of BDR is obtained as 496675. This high value of BDR indicates that the antenna is capable over a wide frequency range of operation with comparatively smaller dimension.

It is observed from Table 1 that the lower edge frequency of SWB operation is the lowest for the proposed antenna design. Therefore, it provides the highest ratio bandwidth and bandwidth in percentage. As the lower edge frequency is minimum the corresponding wavelength is maximum. Therefore, the corresponding electrical dimension of the proposed antenna design is also the smallest. So in Eq. (3) of BDR numerator is maximized, and denominator is minimized. As a result, the proposed design exhibits higher value of BDR than other reported antenna structures.

The E plane and H plane normalized radiation patterns of the proposed SWB antenna are depicted in Figure 11. Nearly dipole like radiation pattern in E plane (x-z plane) and omnidirectional radiation pattern in H plane (y-z plane) are obtained for comparatively lower frequency of operation. As the frequency of operation increases the pattern resembles distorted omnidirectional nature in both planes. These distortions are observed at higher frequencies due to the excitation of higher order modes at those frequencies [18].

The measured peak gain values at some discrete frequencies of this antenna are plotted in Figure 12. It shows that the antenna has a moderate satisfactory gain over the entire frequency range of SWB operation with maximum gain of 7.5 dBi.

Table 1. Comparison of proposed design with the reported SWB antennas.

Ref.	Antenna Dimension (Electrical)	Lower edge frequency of band (GHz)	Ratio Bandwidth	Bandwidth (%)	BDR
[2]	$0.19\lambda\times0.16\lambda$	0.41	21.6 : 1	182.30	5997
[3]	$0.43\lambda\times0.45\lambda$	1.08	25 : 1	184.83	955.19
[4]	$0.32\lambda\times0.32\lambda$	0.64	25 : 1	184.61	1802.83
[5]	$0.35\lambda\times0.24\lambda$	0.79	21.9 : 1	182.68	2174.76
[6]	$0.26\lambda\times0.28\lambda$	1.05	31 : 1	187.56	2576.37
[7]	$0.18\lambda\times0.22\lambda$	1.30	15.38 : 1	175.58	4261.01
[8]	$0.33\lambda\times0.25\lambda$	2.50	32 : 1	187.87	2277.21
[9]	$0.09\lambda\times0.12\lambda$	0.90	111.1 : 1	196.43	18188.16
[10]	$0.20\lambda\times0.21\lambda$	2.43	13.55 : 1	172.50	4107.14
[11]	$0.16\lambda\times0.13\lambda$	0.96	14.56 : 1	174.29	7468.51
[12]	$0.17\lambda\times0.13\lambda$	0.95	14.52 : 1	174.23	7871.49
[13]	$0.27\lambda\times0.18\lambda$	2.50	11.6 : 1	168.25	3462.02
[14]	$0.16\lambda\times0.27\lambda$	1.42	63.38 : 1	193.70	4483.79
[15]	$0.17\lambda\times0.37\lambda$	1.44	13.06 : 1	172	2735
[16]	$0.033\lambda\times0.033\lambda$	0.50	60 : 1	193	175818
[17]	$0.30\lambda\times0.29\lambda$	4.60	11.31 : 1	168	1903.26
[18]	$0.32\lambda\times0.34\lambda$	3.40	11 : 1	166.67	1531.89
[19]	$0.35\lambda\times0.36\lambda$	1.68	15.48 : 1	175.72	1394.60
[20]	$0.33\lambda\times0.23\lambda$	2.18	20.4 : 1	181.31	2388.80
[21]	$0.26\lambda\times0.25\lambda$	2.75	25.82 : 1	185	2912.24
Proposed Design	$0.02\lambda\times0.02\lambda$	0.10	300 : 1	198.67	496675

4. TIME DOMAIN ANALYSIS

The time domain analysis of Super Wide Band antenna is as essential as frequency domain analysis to study the behavior of the antenna while transmitting and receiving the pulse in time domain. The time domain analysis of the proposed antenna is carried out by using CST MWS simulator for two types of arrangement, i.e., face to face and side by side. The distance between two identical antenna structures is kept at 30 cm for both the cases. To perform the analysis a Gaussian pulse has been chosen for transmitting and receiving purpose. The transmitted pulse and received pulse for both the arrangements are shown in Figure 13. The similarity between transmitted and received pulses is calculated using the following expression of Fidelity Factor (FF) for both arrangements [24].

$$FF = \max\left[\frac{\int_{-\infty}^{\infty} S_t(t)S_r(t+\tau)d\tau}{\sqrt{\int_{-\infty}^{\infty} \mid S_t(t) \mid^2 dt}\sqrt{\int_{-\infty}^{\infty} \mid S_r(t) \mid^2 dt}}\right] \tag{4}$$

In Eq. (4) $S_t(t)$ and $S_r(t)$ are transmitted and received signal, and τ is delay which is varied to maximize numerator. The value of fidelity factor is obtained as 86% for face to face arrangement while for side by side arrangement it is about 80%. Therefore, the signal has smaller amount of distortion in face to face arrangement.

Another critical parameter for SWB antenna is group delay which indicates the far field phase linearity. It is a method of measuring time domain signal distortion introduced by the antenna. The distance between two antenna structures is maintained at 30 cm for face to face and side by side

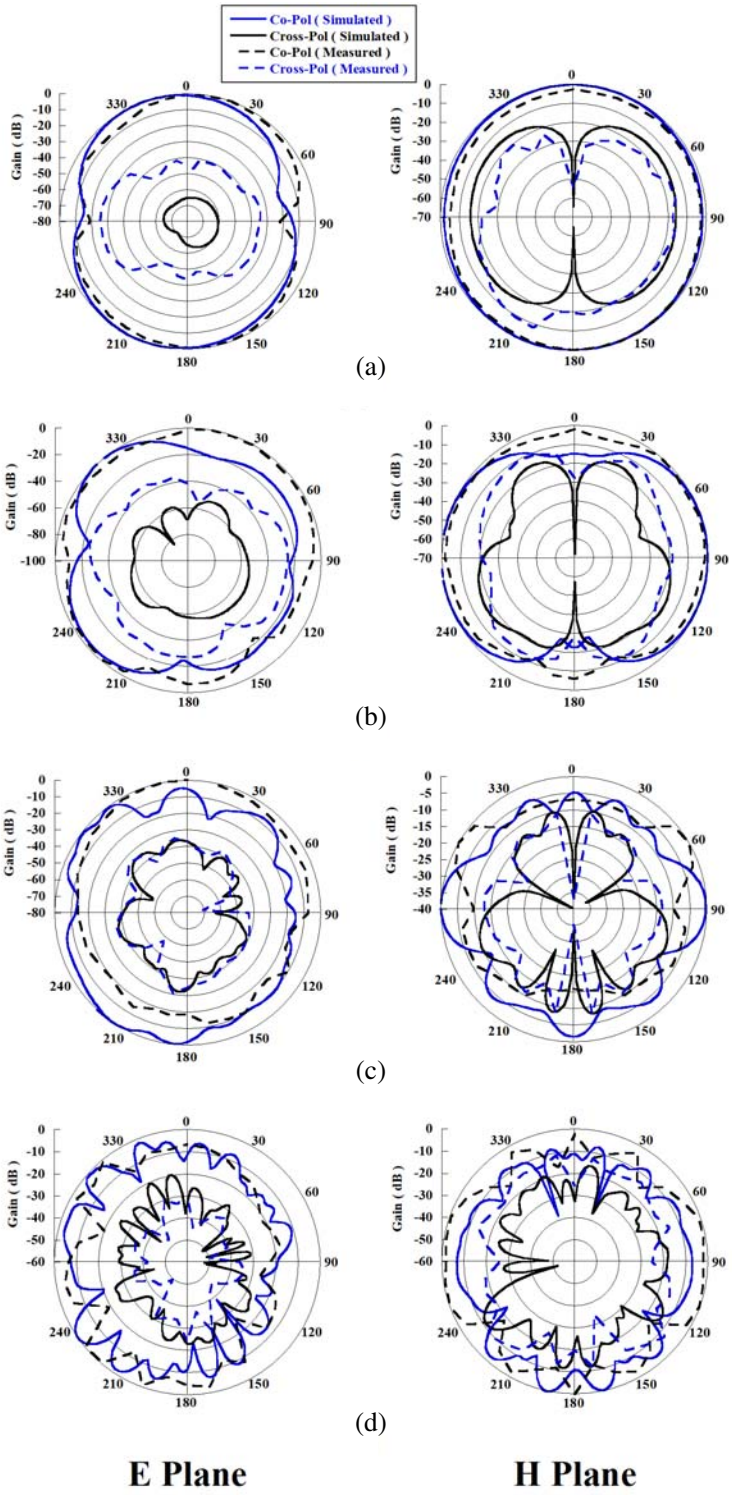

Figure 11. Normalized radiation patterns at (a) 2.21 GHz, (b) 5.89 GHz, (c) 14.1 GHz, (d) 23.6 GHz.

arrangements. As shown in Figure 14 it is clearly observed that the group delay has very small variation (<1nS) for the entire frequency band of SWB operation in both arrangements.

Figure 15 shows magnitude of isolation (S_{21}) for two same arrangements at same distance as described earlier. It is observed that isolation is greater than 30 dB for both arrangements over the

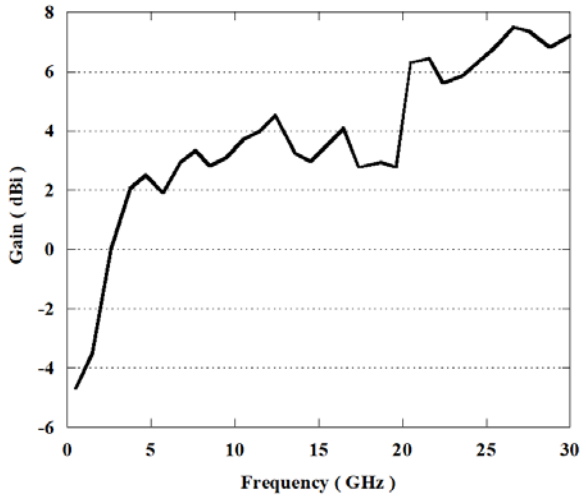

Figure 12. Measured gain vs. frequency plot of the proposed SWB antenna.

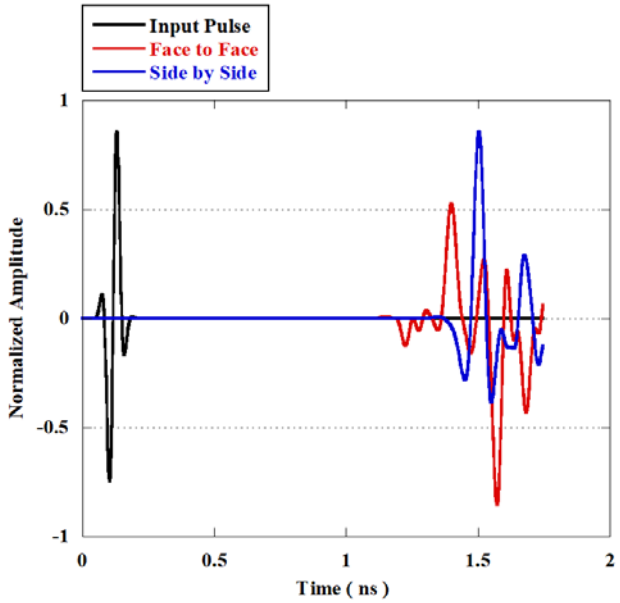

Figure 13. Normalized amplitude of input and received signal for two different arrangements.

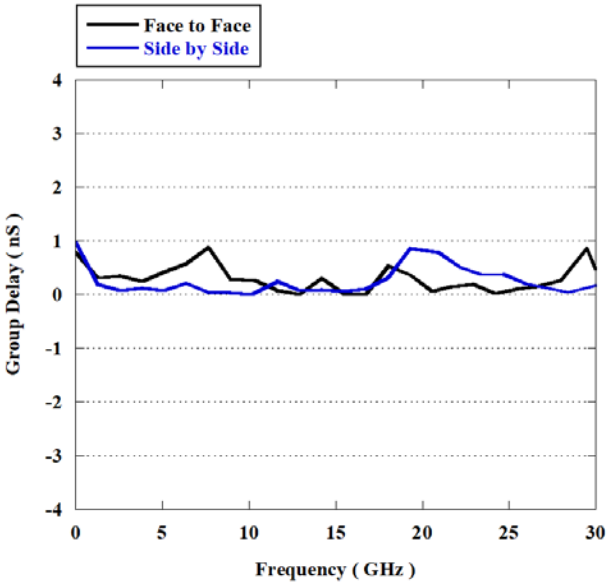

Figure 14. Group delay vs. frequency plot for face to face and side by side arrangements.

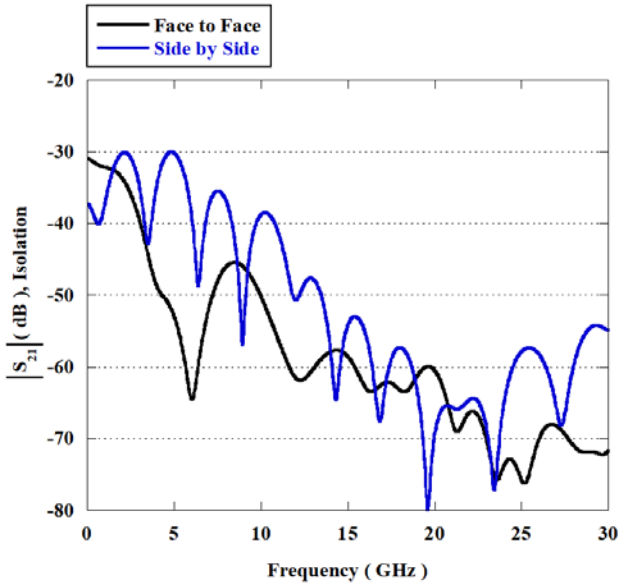

Figure 15. Isolation magnitude, $|\ S_{21}\ |$ against frequency characteristics for face to face and side by side arrangements.

entire frequency band of operation. High value of isolation indicates uncorrelated pulse transmission from both the ports in each arrangement. Variations of phase of S_{21} for both arrangements are shown in Figure 16. The linear variations of phase for both arrangements specify the absence of any out of phase component in the received signal.

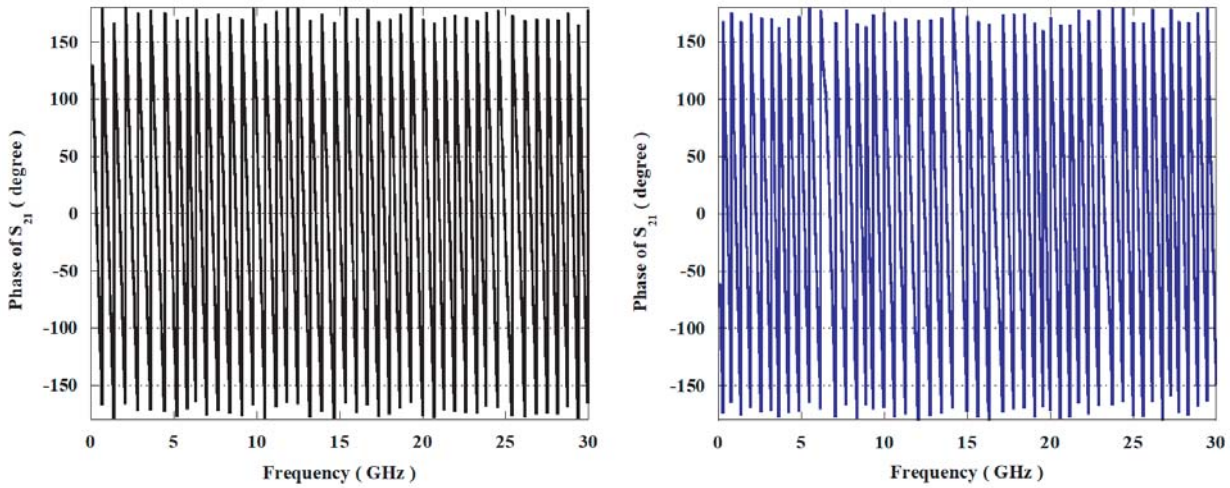

Figure 16. Phase of S_{21} against frequency characteristics for (a) face to face arrangement, (b) side by side arrangement.

5. CONCLUSION

A microstrip line fed staircase fractal loaded corner modified square patch planar antenna has been presented for Super Wide Band operation. The miniaturization property of fractal curve is properly utilized to bring down the lower edge frequency of operation. As a result, the value of Bandwidth Dimension Ratio becomes very high as compared to the other SWB antenna designs available in literature. Therefore, the antenna is capable of operating over a wide band with smaller dimension. Far field radiation characteristics are also observed for the proposed SWB antenna. Time domain analysis also confirms its application as SWB antenna. As the antenna supports a wide bandwidth from 0.1 GHz to 30 GHz it is suitable for different wireless applications like Amateur Radio (1.2 GHz), LTE (1.9/2.5 GHz), Digital Audio Broadcasting (1.9 GHz), ISM (2.45 GHz), Wi-Fi (2.4 GHz), GPS (1.2/1.5 GHz), WIMAX (3.3 GHz–3.7 GHz), WLAN (2.5/5.2 GHz), Broadband Disaster Relief (4.9 GHz), UWB (3.1GHz–10.6 GHz) operation, Radio Astronomy (22.5 GHz, 24.05 GHz–27 GHz), Short Range Radar (21.4 GHz–27 GHz), etc.

REFERENCES

1. Tran, D., P. Aubry, A. Szilagyi, I. E. Lager, O. Yarovyi, and L. P. Ligthart, *On the Design of a Super Wide Band Antenna, Ultrawide Band*, Intech Open, 2010.
2. Liang, X.-L., S.-S. Zhong, and W. Wang, "Elliptically planar monopole antenna with extremely wide bandwidth," *Electronics Letters*, Vol. 42, No. 8, 441–442, 2006.
3. Liu, J., K. P. Esselle, S. G. Hay, and S. Zhong, "Achieving ratio bandwidth of 25 : 1 from a printed antenna using a tapered semi-ring feed," *IEEE Antennas and Wireless Propagation Letters*, Vol. 10, 1333–1336, 2011.
4. Dong, Y., W. Hong, L. Liu, Y. Zhang, and Z. Kuai, "Performance analysis of a printed super-wideband antenna," *Microwave and Optical Technology Letters*, Vol. 51, No. 4, 949–956, 2009.
5. Barbarino, S. and F. Consoli, "Study on super-wideband planar asymmetrical dipole antennas of circular shape," *IEEE Transactions on Antennas and Propagation*, Vol. 58, No. 12, 4074–4078, 2010.
6. Liu, J., K. P. Esselle, S. G. Hay, and S. Zhong, "Compact super-wideband asymmetric monopole antenna with dual-branch feed for bandwidth enhacement," *Electronics Letters*, Vol. 49, No. 8, 515–516, 2013.

7. Samsuzzaman, M. and M. T. Islam, "A semicircular shaped super wide band patch antenna with high bandwidth dimension ratio," *Microwave and Optical Technology Letters*, Vol. 57, No. 2, 445–452, 2015.
8. Manohar, M., R. S. Kshetrimayum, and A. K. Gogoi, "Printed monopole antenna with tapered feedline, feed region and patch for super wide band applications," *IET Microwaves Antennas and Propagation*, Vol. 8, No. 1, 39–45, 2014.
9. Manohar, M., R. S. Kshetrimayum, and A. K. Gogoi, "Super wideband antenna with single band suppression," *International Journal of Microwave and Wireless Technologies*, Vol. 9, No. 1, 143–150, 2017.
10. Aziz, S. Z. and M. F. Jamlos, "Compact super wideband patch antenna design using diversities of reactive loaded technique," *Microwave and Optical Technology Letters*, Vol. 58, No. 12, 2811–2814, 2016.
11. Okas, P., A. Sharma, and R. K. Gangwar, "Circular base loaded modified rectangular monopole radiator for super wideband application," *Microwave and Optical Technology Letters*, Vol. 59, No. 10, 2421–2428, 2017.
12. Okas, P., A. Sharma, and R. K. Gangwar, "Super-wideband CPW fed modified square monopole antenna with stabilized radiation characteristics," *Microwave and Optical Technology Letters*, Vol. 60, No. 3, 568–575, 2018.
13. Rahman, M. N., M. T. Islam, M. Z. Mahmud, and M. Samsuzzaman, "Compact microstrip patch antenna proclaiming super wideband characteristics," *Microwave and Optical Technology Letters*, Vol. 59, No. 10, 2563–2570, 2017.
14. Rahman, S.U., Q. Cao, H. Ullah, and H. Khalil, "Compact design of trapezoid shape monopole antenna for SWB application," *Microwave and Optical Technology Letters*, Vol. 61, No. 8, 1931–1937, 2019.
15. Chen, K.-R., C.-Y.-D. Sim, and J.-S. Row, "A compact monopole antenna for super wideband applications," *IEEE Antennas and Wireless Propagation Letters*, Vol. 10, 488–491, 2011.
16. Waladi, V., N. Mohammadi, Y. Zehforoosh, A. Habashi, and J. Nourinia, "A novel modified star-triangular fractal (MSTF) monopole antenna for super-wideband applications," *IEEE Antennas and Wireless Propagation Letters*, Vol. 12, 651–654, 2013.
17. Singhal, S. and A. K. Singh, "Modified star-star fractal (MSSF) super-wideband antenna," *Microwave and Optical Technology Letters*, Vol. 59, No. 3, 624–630, 2017.
18. Singhal, S. and A. K. Singh, "CPW fed hexagonal Sierpinski super wideband fractal antenna," *IET Microwaves Antennas and Propagation*, Vol. 10, No. 15, 1701–1707, 2016.
19. Figueroa-Torres, C. A., J. L. Medina-Monroy, H. Lobato-Morales, R. A. Chavez-Perez, and A. Calvillo-Tellez, "A novel fractal antenna based on the Sierpinski structure for super wide-band applications," *Microwave and Optical Technology Letters*, Vol. 59, No. 5, 1148–1153, 2017.
20. Dorostkar, M. A., M. T. Islam, and R. Azim, "Design of a novel super wide band circular-hexagonal fractal antenna," *Progress In Electromagnetics Research*, Vol. 139, 229–245, 2013.
21. Singhal, S. and A. K. Singh, "Asymmetrically CPW-fed circle inscribed hexagonal super wideband fractal antenna," *Microwave and Optical Technology Letters*, Vol. 58, No. 12, 2794–2799, 2016.
22. Darimireddy, N. K., R. R. Reddy, and A. M. Prasad, "A miniaturized hexagonal-triangular fractal antenna for wide-band applications," *IEEE Antennas and Propagation Magazine*, Vol. 60, No. 2, 104–110, 2018.
23. Dastranj, A., F. Ranjbar, and M. Bornapour, "A new compact circular shape fractal antenna for broadband wireless communication applications," *Progress In Electromagnetics Research C*, Vol. 93, 19–28, 2019.
24. Quintero, G., J.-F. Zurcher, and A. K. Skrivervik, "System fidelity factor: A new method for comparing UWB antennas," *IEEE Transactions on Antennas and Propagation*, Vol. 59, No. 7, 2502–2512, 2011.